Draft version March 9, 2020
Typeset using LaTeX **manuscript** style in AASTeX62

Exercises in Mainline Stellar Nuclear Burning

Ansh Sehgal[1]

[1] *Department of Physics and Astronomy, Clemson University, Clemson, SC 29634-0978*

ABSTRACT

We examine the life cycle of a star by decomposing its nucleosynthesis into distinct burning stages, or "shells" to better understand the underlying processes in stellar interiors. We run calculations at increasing temperatures and densities, until the formation of metallic elements like Iron, signaling the exhaustion of the initial stellar nuclear fuel.

1. INTRODUCTION

Stellar nucleosynthesis follows a fairly well-understood sequence of burning stages. These are reviewed in a several text books, including Clayton (1983); Arnett (1996); Iliadis (2007). The purpose of this brief paper is to present a set of computational exercises using NucNet Tools to demonstrate these stages in a massive star.

Together we will walk through the basic stages of element fusion inside of stars, from Hydrogen and Helium to the more metallic ones such as Iron and Nickel.

2. METHODS

We use the docker repository for the nucleosynthesis code found in :

docker single-zone

To run, use a command like:

```
docker run -it -v ${PWD}/work/input:/input_directory -v ${PWD}/work/output:/
   output_directory -e VAR="@run_h.rsp" single_zone:default
```

where *run_h.rsp* reads

```
--t9_0 0.03 --rho_0 50.
```

```
--network_xml /input_directory/data_pub/my_net.xml
--zone_xml /input_directory/data_pub/Lodders.xml
--nuc_xpath "[z <= 94]" --iterative_solver gmres --iterative_t9 2
--output_xml /output_directory/out.xml --tend 3.15e15
```

But we will edit the response file to update the increasing temperature and density at every new burning stage.

3. HYDROGEN BURNING

The first stellar burning phase is hydrogen burning, which converts abundant hydrogen into helium. In a massive star this occurs at higher temperature but lower density than in the Sun.

Plotted below is the mass fraction of the Hydrogen and resulting Helium that is generated due to the pp chain reaction:

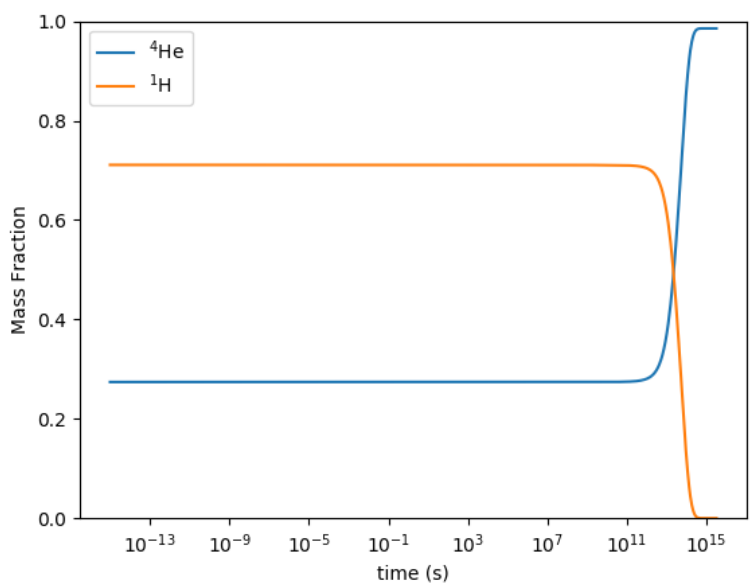

Figure 1. log plot of ^{1}H and ^{4}He as a function of time

We can also examine the abundances of the Carbon, Neon and Oxygen isotopes during the CNO cycle:

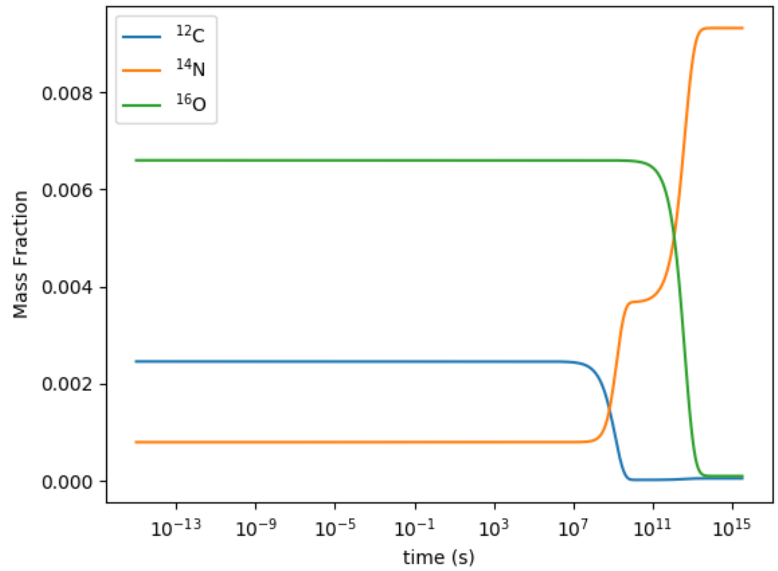

Figure 2. log plot of ^{12}C,^{14}N, and ^{16}O as a function of time

As we see, there is a buildup of ^{14}N which can be attributed to the rather slow reaction time of the process, which comes after. Namely:

$$^{14}N \rightarrow ^{15}O + \gamma \tag{1}$$

Because this reaction is so slow, there is a natural saturation of Nitrogen that occurs.

4. HELIUM BURNING

Once a star burns hydrogen to helium, it contracts and heats until the He ignites. The He burns to C and O (but not much Ne as we see below)

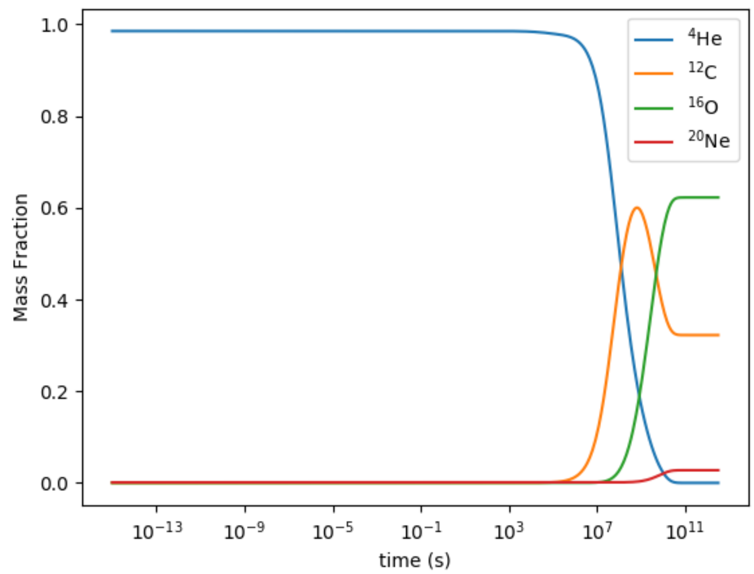

Figure 3. log plot of ^{4}He,^{12}C, ^{16}O as a function of time. $^{20]}$Ne is also plotted to show that Oxygen is really the stopping point for the triple alpha process

In this triple-α process, the ^{4}He 's combine together until they form Carbon and Oxygen, leading to the eventual buildup of the ^{16}O seen in the plot. However, ^{20}Ne is not formed as much, due to the fact that the energy needed to overcome the stability of the Oxygen, and the subsequent Coulomb barrier is too much. Only at extreme temperatures (closer to the core) do these elements start to form.

We now wish to consider the s-process (”slow”) in Helium burning.

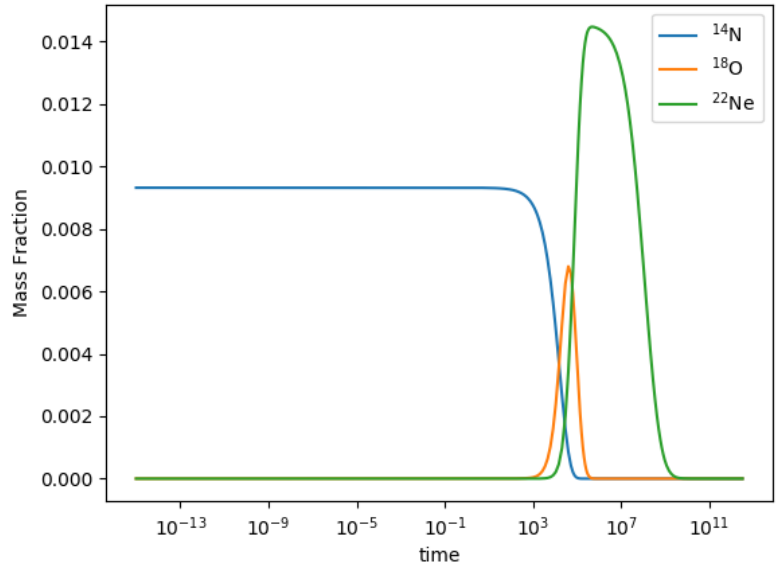

Figure 4. log plot of ^{14}N,^{18}O, ^{22}Ne as a function of time.

The Nitrogen slowly combines with alpha particles to form ^{18}O, which can then combine with more Helium to form the ^{22}Ne.

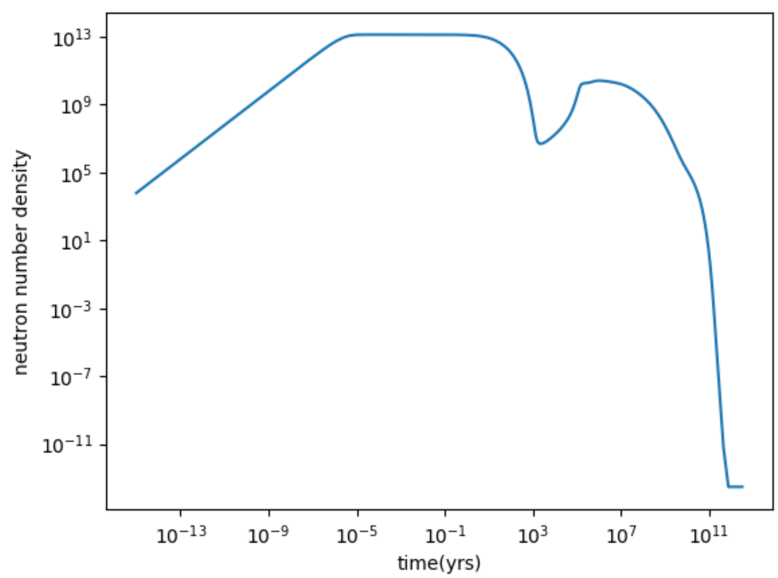

Figure 5. Neutron Number Density as a function of time, on a log-log scale

Here we plot the number density of neutrons over time. In particular, there is a short burst from the reaction:

$$^{13}C +^{4} He \rightarrow^{16} O + n \tag{2}$$

The products include a neutron, leading to the increase of n_n. Then, there is a more steady supply once the ^{22}Ne has formed as mentioned above.

Finally, we examine the abundances of each element at the beginning and end of the calculation to see the evolution of the composition of the star.

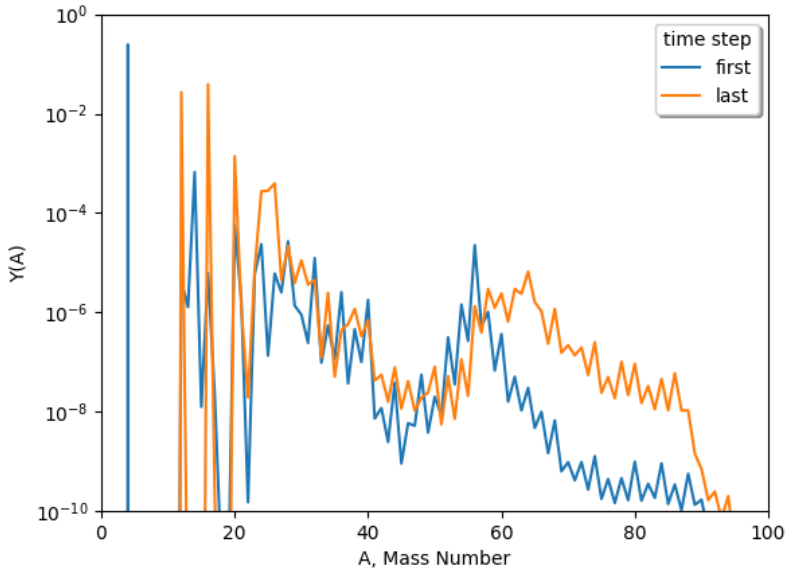

Notice how the final calculation yields higher abundances of heavier elements, which is to be expected given that the hydrogen and helium is being depleted to fuse more metallic elements. The graph spikes right around Carbon and Oxygen, as we expect.

5. CARBON BURNING

The principal products of helium burning are ^{12}C and ^{16}O. As the star contracts and heats, carbon burning begins.

The key reactions that take place are:

$$^{12}C +^{12} C \rightarrow^{24} Mg^{*} \rightarrow^{24} Mg + \gamma \tag{3}$$

$$\rightarrow^{20} Ne +^{4} He \tag{4}$$

$$\rightarrow^{23} Na + p \tag{5}$$

$$^{12}C +^{16} O \rightarrow^{24} Mg +^{4} He \tag{6}$$

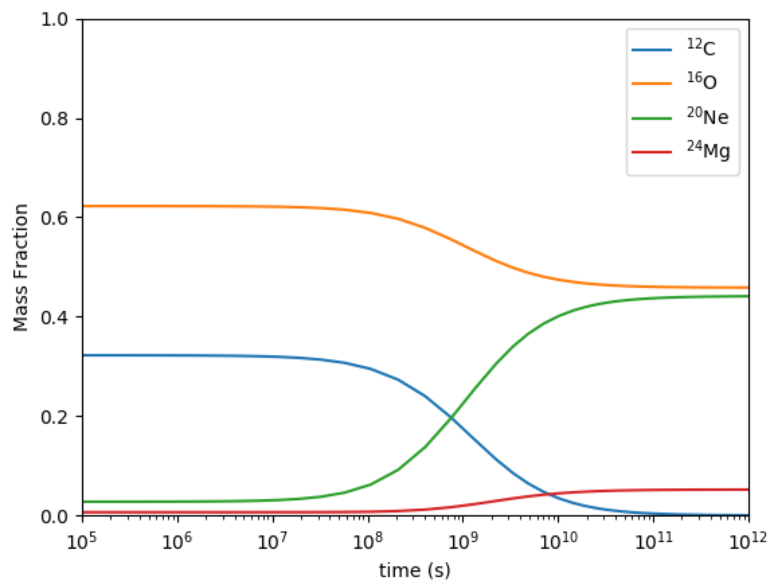

Figure 6. Mass Fraction of the various relevant isotopes to Carbon Burning as a function of time

Notice that as the ^{12}C and ^{16}O is used up in the aforementioned reaction, there is a commensurate rise in the ^{20}Ne and ^{24}Mg

Also note that if the star forms a white dwarf after this burning, it will be a O/Ne/Mg white dwarf, not a C/O white dwarf, as it would have been after helium burning.

6. NEON BURNING

Following carbon burning, the star will contract, heat, and undergo neon burning. This burning stage comprises $^{20}\mathrm{Ne}+\gamma \rightarrow^{16} \mathrm{O}+^{4}\mathrm{He}$ and $^{20}\mathrm{Ne}+^{4}\mathrm{He} \rightarrow^{24} \mathrm{Mg}+\gamma$, which effectively is $^{20}\mathrm{Ne}+^{20}\mathrm{Ne} \rightarrow^{16} \mathrm{O} +^{24} \mathrm{Mg}$.

We run the calculation for 1000 years at an increased ρ and T_9 and find the following abundances

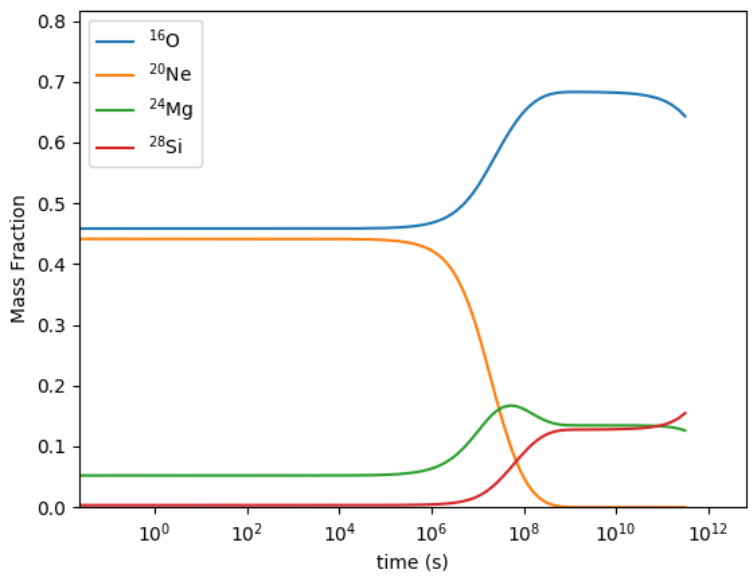

Figure 7. Mass Fraction of the various relevant isotopes to Neon Burning as a function of time

These match our predictions from the reaction equations above; in particular, the rise of ^{16}O and subsequent depletion of ^{20}Ne

7. OXYGEN BURNING

After neon burning, the next stage is oxygen burning. The principal reaction is $^{16}\mathrm{O} +^{16} \mathrm{O} \rightarrow^{32} \mathrm{S}^*$. The excited ^{32}S nucleus then de-excites mostly to ^{28}Si (and an alpha) or ^{32}S.

This is represented in our mass fractions:

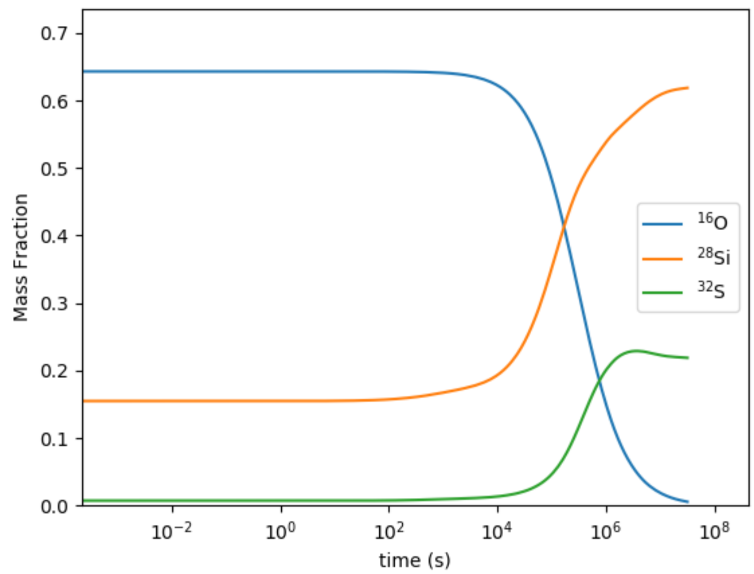

Figure 8. Mass Fraction of the various relevant isotopes to Oxygen Burning as a function of time

We run the calculation for a $T_9 = 2.1$ and $\rho = 1.5 \times 10^6$ g/cc for one year.

Also occurring during oxygen burning is the "gamma" process. The initially present heavy nuclei are disintegrated. First neutrons then protons and alphas are emitted. The nuclei "flow" down the proton-rich side of the stable nuclei. If this matter "freezes out", proton-rich nuclei are formed (the so-called "p-nuclei").

We take a look at the overall abundances as a function of mass number between the initial and final calculation. The overplotting gives a sense of the time evolution.

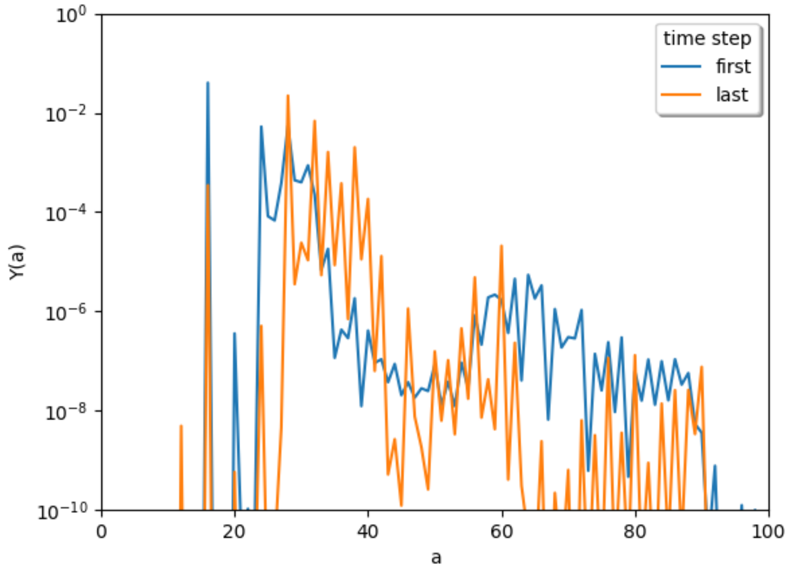

Figure 9. Abundances versus corresponding atomic number, at both the initial and final calculation time step

Note how nuclei "melt" towards the iron-group region.

8. SILICON BURNING

The final mainline burning stage is Si burning. Here ^{28}Si converts to ^{56}Ni, which decays to ^{56}Fe. The burning proceeds through a complicated sequence–some Si disintegrates and the light particles that result capture onto the remaining Si to create heavier nuclei. In fact the burning proceeds through a quasi-equilibrium Bodansky et al. (1968); Meyer et al. (1998).

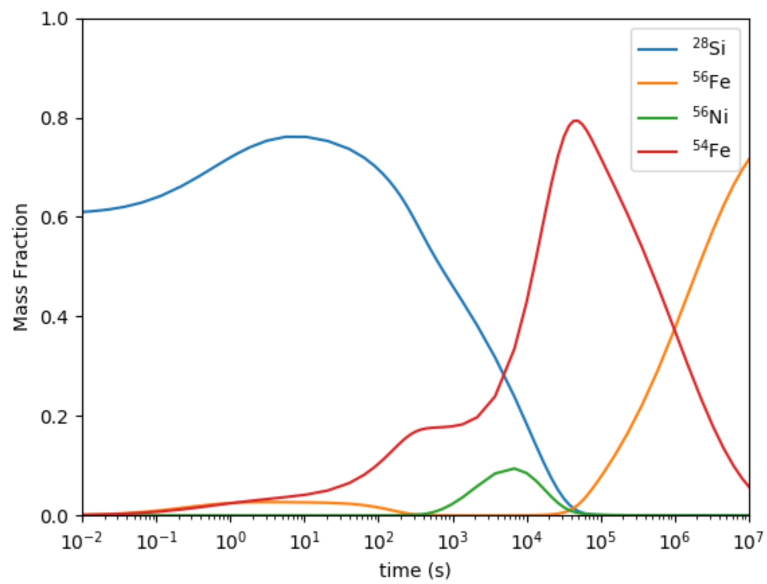

Figure 10. Mass Fraction of the various relevant isotopes to Silicon Burning as a function of time

Now the star has contracted to an extreme level, with $T_9 = 3.5$ and $\rho = 1.5e7$ g/cc in our 1 year calculation.

You might be surprised that the abundance of ^{56}Ni is never particularly large. The reason is that the silicon burning is sufficiently slow that weak decays have time to occur during the burning and thus change the neutron richness of the nuclei present. Also, at this temperature, there is a preference for ^{54}Fe and two protons over ^{56}Ni, as evidence by its relatively high abundance.

9. CONCLUSION

Of course stellar burning really occurs in the context of an evolving star. The temperature and density are not constant, as treated in these exercises, but rather evolve as nuclear fuel is consumed. Furthermore, in many cases, stellar layers are convective, which tends to mix the composition of those layers during the burning. Nevertheless, we hope that by carrying out the above exercises, one will get a good sense of the nature of the mainline stellar burning phases.

REFERENCES

Arnett, D. 1996, Supernovae and nucleosynthesis. an investigation of the history of matter, from the Big Bang to the present (Princeton series in astrophysics, Princeton, NJ: Princeton University Press, c1996)

Bodansky, D., Clayton, D. D., & Fowler, W. A. 1968, ApJS, 16, 299

Clayton, D. D. 1983, Principles of stellar evolution and nucleosynthesis (Chicago: University of Chicago Press, 1983)

Iliadis, C. 2007, Nuclear Physics of Stars (Wiley-VCH Verlag)

Meyer, B. S., Krishnan, T. D., & Clayton, D. D. 1998, ApJ, 498, 808